LITHOSPHERIC STRESS AND BASALTIC MAGMA ASCENT ON THE MOON, WITH IMPLICATIONS FOR LARGE VOLCANIC PROVINCES AND EDIFICES.

P. J. McGovern[1] and M. M. Litherland[2], [1]Lunar and Planetary Institute, Universities Space Research Association, 3600 Bay Area Blvd., Houston, TX 77058 (mcgovern@lpi.usra.edu), [2]Department of Geophysics, Stanford University, Stanford, CA 94305 (mairi@stanford.edu).

Introduction: The broad expanses of basaltic volcanic plains on the Moon, the maria, are a primary manifestation of lunar magmatic and thermal evolution. Enormous volumes of basalt fill most of the largest impact basins on the lunar nearside, and also cover regions of varying elevation around and between basins. Controls on the distribution of mare units are not well understood: difficulties such as the eruption of high-density (high-TiO_2) units on elevated terrain in Oceanus Procellarum and Mare Tranquilitatis elude explanation within the traditional framework of buoyancy. Here we show that the mechanical response of the lunar lithosphere to the initial filling of basins creates a combination of flexural and membrane stress components, inducing a pressure distribution on vertical conduits (dikes) that is particularly favorable to magma ascent; this condition occurs only in an annular region around large circular loads. We argue that this “magma pump” effect exerts strong control on the spatial distribution and observed compositions of basalt flows, the former by facilitating the formation of large volcanic edifices [1], the latter by allowing dense magmas to ascend from the mantle to the surface.

Loading Models: We use an analytic loading solution [2] that includes both flexural and membrane support to calculate deflections and stresses of an elastic lithosphere from initial basin-filling mare loads [e.g., 2-4]. The loading stresses are used to predict subsequent locations of favored magma ascent based on two criteria: stress orientations at the top and bottom of the lithosphere (horizontal extension [5]) and stress gradients throughout the lithosphere (extension increasing upwards [6]). For small planets like the Moon, the effects of membrane stresses (constant through the thickness of the lithosphere) can place segments of the lithosphere into extension with positive stress gradients from flexure, accomplishing the difficult feat of satisfying both ascent criteria simultaneously [e.g., 7, 8].

We use lithospheric stress gradients to calculate magma ascent rates. The equation for ascent velocity in a dike of width w is [6, combining equations]:

$$u_z = (1/3\,\eta)\, w^2\, (d\Delta\sigma_y/dz + d\Delta P/dz - \Delta\rho\, g) \qquad (1)$$

where η is magma viscosity, $d\Delta\sigma_y/dz$ is the stress gradient, also called the vertical gradient in tectonic stress (or VGTS), $d\Delta P/dz$ is the gradient in overpressure, and $-\Delta\rho\, g$ is magma buoyancy (g is negative in our coordinate system so buoyancy increases u_z). We can equate the first and third terms on the right side of Eqn. 1 to estimate the adverse density contrast (magma denser than country rock) that can be overcome by the VGTS contribution (Fig. 2), allowing eruption. Other favorable effects (e.g., volatile exsolution) may also contribute to positive u_z in the uppermost lithosphere.

Trans-Imbrium Volcanic Zone: The pairs of red and white lines in Fig. 1 enclose annular regions where both ascent criteria are satisfied by Imbrium-induced loading stresses, for elastic lithosphere thicknesses T_e = 50 and 75 km [early stage Imbrium loading of 4], respectively. Note that four proposed volcanic edifices [1] occur near the dashed lines that indicate the maximum magma ascent enhancement; the two more distal edifices may have been affected by later Imbrium load phases with higher T_e [4] that would push the lines outward (while reducing the VGTS effect). A number of locations where olivine was detected [9] also fall within the favored annuli, suggesting that stress-assisted ascent of olivine-rich cumulates, either directly from the mantle or in mid-crustal reservoirs, is responsible (although an ejecta origin is also possible).

Application to Tranquilitatis (Basin?) and Cauchy (Shield?): The development of the Tranquilitatis region can be examined by superposing loading solutions for the surrounding basins. Much of Tranquitatis is characterized by high TiO_2 content (Fig. 2), indicating high magma densities. Western Mare Tranquilitatis occupies a topographic trough, whereas the eastern part consists of an elongated rise (dubbed the Cauchy shield by [1]) aligned roughly between the Maria Serenitatis and Fecunditatis, with superposed graben (Rimae Cauchy) sharing that alignment. The superposed loading solutions in Fig. 2 show a broad zone of enhanced magma ascent in Tranquilitatis with density offsets often exceeding 100 kg/m^3, allowing for ascent of negatively buoyant magmas through the crust. The predicted intrusive alignments are consistent with the observed orientations of Rimae Cauchy and distributions of small cones and shields [10].

Scenarios for development of the proposed Cauchy edifice [1] can be constrained by remote sensing. Cauchy lacks a strong corresponding free-air gravity high characteristic of flexurally supported shield volcanoes, but joint analysis of gravity and topography indicates a distinct local crustal thickness maximum beneath the structure [11], consistent with an isostatically compensated rise of crustal-density material. Mapping and interpretation of imaging data indicate that the surface basalts in Eastern Tranquilitatis are only several hundred meters in thickness [12], a fraction of the observed 2.1

km relief [1]. Perhaps the basalts are a thin carapace covering a pre-existing crustal block. Alternatively, the rise could have been built up by substantial amounts of intrusion and underplating of moderate-density magmas, with late-stage eruptions of denser cumulate-rich magmas aided by the VGTS effect. The former case is inconsistent with a proto-Tranquilitatis basin, while the latter allows it.

Distributions of Volcanic Provinces and Constructs: Two primary conditions for magma ascent must be met: 1) the presence of the magma, and 2) the mechanical conditions that allow ascent through the lithosphere. Condition 1 may be controlled by the distribution of heat-producing elements, accounting for the strong preference of the mare toward the lunar nearside [e.g., 13], although impact-related heating may also play a role [14]. Farside basins, lacking substantial magmas to supply even the initial basin infill, will not trigger the VGTS effect. Condition 2 will tend to become more difficult to satisfy with time, due to increasing bias toward lithospheric compression as the Moon cools [e.g., 15]. Under such a regime, volcanism remains possible only where a favorable stress regime counteracts compression. Thus, we argue that the locations of prominent (and in many cases, young) volcanic provinces and edifices in the regions flanking the largest mare basin-filling loads on the Moon are not coincidences, but rather results of the magma ascent-enhancing stress state found at the basins' margins.

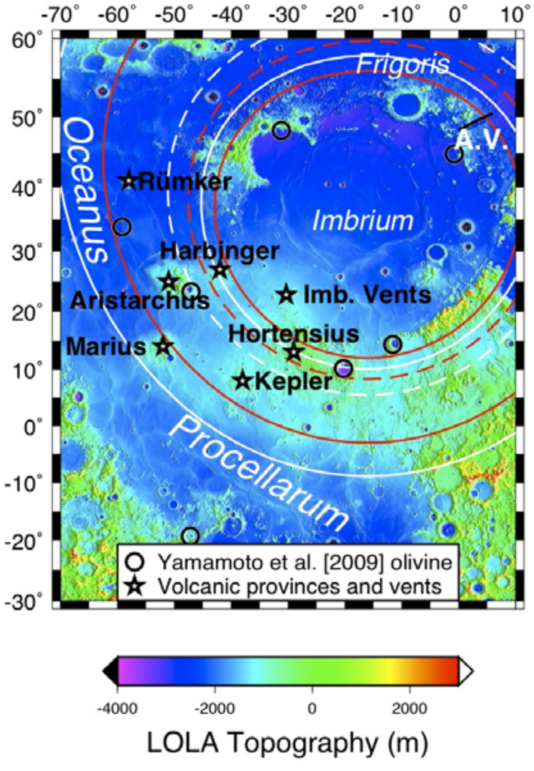

Figure 1: Shaded relief map of lunar nearside near Imbrium, using LOLA topography [16]. Stars show locations of proposed lunar shield volcanoes [1] and late-stage source vents for Imbrium-filling flows [17]. Black circles show olivine detections [9]. Red and white circles delineate favored ascent zones for "young" Imbrium mare loads [5] for $T_e = 50$ and 75 km, respectively, calculated from shallow spherical shell loading models [3]. Solid lines indicate inner and outer boundaries of ascent zone, dashed lines indicate maximum ascent velocity (and density offset).

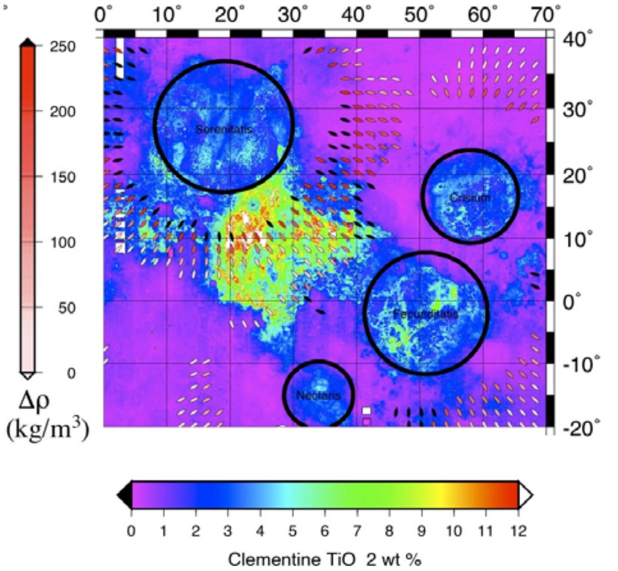

Figure 2: Principal stress orientations for superposition of basin loading stresses (as above) from Serenitatis, Nectaris, Fecunditatis, and Crisium basins, on basemap of lunar TiO_2 model from Clementine spectral data [18] (bottom colorbar). Linear stress symbols are aligned perpendicular to the least compressive principal stress in the lithosphere (demonstrating the orientations of associated dikes), and are plotted only where two conditions are met: extension at both the top and bottom of lithosphere, and principal stress orientations are within 20° at the bottom and top of the lithosphere. Symbol colors (shades of red) show the equivalent density offset $\Delta\rho$ (left colorbar) provided by the positive VGTS (eq. 1). Load margins shown by solid circles.

References: [1] Spudis P. D. et al. (2011) *LPS XLII* (this volume). [2] Brotchie J. F. and Sylvester R. (1969) *JGR, 74*, 5240. [3] Solomon S. C. and Head J. W. (1979) *JGR, 84*, 1667. [4] Solomon S. C. and Head J. W. (1980) *Rev. Geophys. and Space Phys., 18*, 107-141. [5] Anderson, E. M. (1936) *Proc. R. Soc. Edinburgh, 56*, 128. [6] Rubin A. M. (1995) *Annu. Rev. Earth Planet. Sci., 23*, 287, 1995. [7] Rumpf M. E., and McGovern P. J. (2007) *LPS XXXVIII*, Abstract # 1374. [8] Litherland M. M. and McGovern P. J. (2009) *LPS XL*, Abstract # 2201. [9] Yamamoto S. et al. (2010) Nature Geoscience DOI: 10.1038/NGEO897. [10] Guest J.E. and Murray J.B. (1976) *J. Geol. Soc. (London) 132*, 251. [11] Neumann, G. A. et al (1996) *JGR 101*, 16,841. [12] Rajmon D. and Spudis P. (2004) *MAPS 39*, 1699. [13] Wieczorek, M. A. and Phillips R. J. (2000) *JGR 105*, 20,417. [14] Elkins-Tanton L. T. et al. (2004) *EPSL 222*, 17. [15] Watters, T. R. et al (2010), Science, 329, 936. [16] Smith D.E. *et al*. (2010) *GRL 37*, L18204. [17] Schaber, G. G. (1973) *Proc. LSC 4*, 73. [18] Gillis J. J. et al (2004) *Geochimica, 68*, 3791.